Annals of Botany Page 1 of 9
doi:10.1093/aob/mct259, available online at www.aob.oxfordjournals.org

ANNALS OF BOTANY
Founded 1887

Root cortical aerenchyma inhibits radial nutrient transport in maize (*Zea mays*)

Bo Hu[1,2], Amelia Henry[3], Kathleen M. Brown[1,3] and Jonathan P. Lynch[1,3,*]

[1]*Department of Plant Science, The Pennsylvania State University, University Park, PA 16802, USA,* [2]*Agriculture Department, Inner Mongolia Agriculture University, Hohhot, P. R. China and* [3]*Intercollege Program in Plant Biology, The Pennsylvania State University, University Park, PA 16802, USA*
** For correspondence. E-mail jpl4@psu.edu*

Received: 30 June 2013 Returned for revision: 5 August 2013 Accepted: 11 September 2013

• *Background and Aims* Formation of root cortical aerenchyma (RCA) can be induced by nutrient deficiency. In species adapted to aerobic soil conditions, this response is adaptive by reducing root maintenance requirements, thereby permitting greater soil exploration. One trade-off of RCA formation may be reduced radial transport of nutrients due to reduction in living cortical tissue. To test this hypothesis, radial nutrient transport in intact roots of maize (*Zea mays*) was investigated in two radiolabelling experiments employing genotypes with contrasting RCA.
• *Methods* In the first experiment, time-course dynamics of phosphate loading into the xylem were measured from excised nodal roots that varied in RCA formation. In the second experiment, uptake of phosphate, calcium and sulphate was measured in seminal roots of intact young plants in which variation in RCA was induced by treatments altering ethylene action or genetic differences.
• *Key Results* In each of three paired genotype comparisons, the rate of phosphate exudation of high-RCA genotypes was significantly less than that of low-RCA genotypes. In the second experiment, radial nutrient transport of phosphate and calcium was negatively correlated with the extent of RCA for some genotypes.
• *Conclusions* The results support the hypothesis that RCA can reduce radial transport of some nutrients in some genotypes, which could be an important trade-off of this trait.

Key words: Aerenchyma, radial transport, root, nutrient uptake, phosphorus, sulfur, calcium, maize, *Zea mays*.

INTRODUCTION

Root cortical aerenchyma (RCA) in maize is formed by programmed cell death of cortical cells, leaving air-filled lacunae (Esau, 1977). RCA is induced by a variety of stimuli, including hypoxia, nutrient deficiency, mechanical impedance and drought (Drew *et al.*, 1980, 2000; He *et al.*, 1996; Bouranis *et al.*, 2003; Zhu *et al.*, 2010). We hypothesized that RCA may be an adaptive response to nutrient stress by reducing the metabolic cost of soil exploration (Lynch and Brown, 1998). In support of this hypothesis, Fan *et al.* (2003) observed a 70 % decrease in respiration of maize (*Zea mays*) aerenchymatous roots compared with non-aerenchymatous roots, and showed that RCA formation was negatively correlated with respiration and tissue phosphorus content when RCA formation was manipulated by genetics, phosphorus availability or ethylene. Similarly, respiration rates were lower in seminal roots of maize genotypes that produced large amounts of RCA under drought stress, and this was associated with greater rooting depth and improved leaf water status, shoot growth and yield (Zhu *et al.*, 2010). Simulations with the structural–functional model *SimRoot* predicted that RCA would increase growth under low phosphorus, potassium or nitrogen stress by remobilizing nutrients from the root cortex and reducing root respiration (Postma and Lynch 2010, 2011).

Trade-offs for RCA formation are not understood, but the presence of genetic variation within maize for this trait suggests that RCA formation confers both benefits and costs. A study of the effect of RCA on root mechanical strength, measured as resistance to radial compression, showed that species with multiseriate rings in the outer cortex, including maize, were not weakened by the presence of flooding-induced RCA, while species lacking multiseriate rings collapsed more readily (Striker *et al.*, 2007). RCA formed under phosphorus deficiency contributed to reduced radial hydraulic conductivity in maize roots (Fan *et al.*, 2007). An additional possible trade-off of RCA formation may be reduced radial transport of nutrients across the cortex, caused by longer path length and reduced cross-sectional area of both apoplastic and symplastic pathways. This study tested this hypothesis by examining the effects of RCA on radial transport of phosphate, calcium and sulphate in maize roots. We used natural genetic variation as well as ethylene and 1-methylcyclopropene (1-MCP) treatments to produce plants with varying RCA. We hypothesized that RCA would decrease radial transport of these nutrients.

MATERIALS AND METHODS

Two sets of experiments were conducted using radiolabelling to measure the effects of RCA on radial nutrient transport in maize: (1) a time-course study using excised roots (experiment 1) and (2) whole-plant studies on nutrient uptake (experiment 2). In experiment 1, six recombinant inbred lines (RILs) with contrasting RCA were used and ^{32}P transport and exudation were measured in a short segment of an excised nodal root. In experiment 2, a range of RCA expression was generated by making use of genetic variation among three RILs and treatments with 1-MCP and ethylene. Segments of intact seminal roots were exposed to ^{45}Ca, ^{32}P or ^{35}S and radioactivity was measured in shoots and nutrient solution to assess nutrient transport.

Plant materials and culture

Recombinant inbred lines (RIL 15, RIL 345, RIL 360, RIL 369, RIL 61, RIL 321 in experiment 1 and RIL 39, RIL 76 and RIL 364 in experiment 2) of maize (*Zea mays*) from the IBM (Intermated B73 × Mo17) population (USDA/ARS Maize Genetics Cooperation Stock Center, Urbana, IL, USA) were selected for this study based on contrasting RCA formation in screening studies. Plant growth conditions were similar in the two experiments. Seeds were surface-sterilized in 50 % bleach (3 % NaOCl), imbibed in a benomyl solution (DuPont, Wilmington DE; 5 g L^{-1} for 3 h in experiment 1; 8 g L^{-1} for 1·5 h in experiment 2), then transferred to germination paper (76 lb, Anchor Paper, St Paul, MN, USA), where they were rolled up and maintained in covered beakers (5 L in experiment 1; 1 L in experiment 2) containing $CaSO_4$ (1 L of 0·5 mM in experiment 1; 150 mL of 0·25 mM in experiment 2) and benomyl (2·5 g L^{-1} in experiment 1; 4 g L^{-1} in experiment 2) at 28 °C (4 days in experiment 1; 6 days in experiment 2) in a dark chamber. In experiment 1, germinated seedlings in rolls were then placed under a fluorescent light (~45 μmol m^{-2} s^{-1}) for 1 day before transplanting to aerated solution culture. Seedlings (12 per container in experiment 1; 24 per container in experiment 2) were transferred to open-cell foam plugs suspended above solution culture tanks (30 L in experiment 1; 100 L in experiment 2) and grown in a greenhouse at The Pennsylvania State University, USA 40·802115, -77·860794. In experiment 1, plants were grown for 12 days during July, when the average temperature was 33 °C, average humidity was 45 % and mid-day solar radiation levels averaged 720 μmol m^{-2} s^{-1}. In experiment 2, plants were grown for 7–8 days in March, when temperatures averaged 29 °C and mid-day solar radiation levels averaged 400 μmol m^{-2} s^{-1}. Ambient light was supplemented with metal halide lamps (~150 μmol m^{-2} s^{-1}; 16 h photoperiod). The nutrient solution (pH 4·5) contained 3 mM KNO_3, 2 mM $Ca(NO_3)_2$, 0·5 mM $MgSO_4$, 0·5 mM $(NH_4)_2SO_4$, 0·5 mM $NH_4H_2PO_4$, 25 μM H_3BO_3, 0·5 μM $CuSO_4$, 50 μM Fe-diethylenetriamine penta acetic acid, ferric–sodium complex (DTPA), 2 μM $MnSO_4$, 0·5 μM $(NH_4)_6Mo_7O_{24}$, 2 μM $ZnSO_4$, 50 μM KCl and 50 μM $FeNH_4SO_4$. In experiment 1, the pH of the nutrient solution was adjusted every 2 days to 5·5 with KOH, and the nutrient solution was replaced entirely every 7 days.

Ethylene and 1-MCP treatments

Root treatments to manipulate RCA production in experiment 2 included a control (air), root-zone ethylene application and root-zone 1-MCP application, applied continuously beginning at seedling transfer to solution culture. Ethylene promotes RCA formation (Evans, 2003), and 1-MCP reduces RCA formation (Fan *et al.*, 2003) by inhibiting ethylene action. Solution culture tanks in the control treatment were bubbled at 30 mL min^{-1} with ambient air. In the ethylene treatment, compressed ethylene (1 μL L^{-1} in air, as used by Gunawardena *et al.* (2001) was bubbled through solution culture tanks at 30 mL min^{-1}. Ethylene concentrations in the headspace of the solution culture tanks were measured periodically by gas chromatography (Hewlett-Packard 6890) and averaged 0·56 ± 0·06 μL L^{-1}. For the 1-MCP treatment, 1-methylcyclopropene (3·8 % active ingredient, Rohm and Haas, Philadelphia, PA, USA) was volatilized by dissolving 0·17 g in 5 mL water in a glass scintillation vial, and then transferred quickly into a 2-L sidearm flask. An open-cell foam plug was used to enclose the mouth of the flask, and the headspace containing 1-MCP gas was bubbled through three 100-L tanks at a rate of 30 mL min^{-1} in each tank to achieve a 1-MCP concentration of 7·7 μL L^{-1} solution, assuming all 1-MCP dissolved in solution. The air pump ran continuously, and the 1-MCP was replenished daily into the sidearm flask.

Radionuclide treatments

Experiment 1: ^{32}P transport dynamics in excised root segments. Experiment 1 was performed to measure the movement of ^{32}P in excised root segments. Pairs of RILs were selected for simultaneous testing based on contrasting RCA phenotypes in previous screening studies. Plants were transferred to a laboratory adjacent to the greenhouse. The apical 8 cm of a first-whorl nodal root was excised and installed in a modified Pitman chamber (Fig. 1A) (Lynch and Läuchli, 1984), permitting treatment of a known length of root (in this case 7·4 mm) with radionuclide. A 10-mm segment of root extended from the 1-mL treatment compartment to the 0·5-mL receiver compartment (Fig. 1A). Silicon grease (Dow Corning, Midland, MI, USA) was used to isolate the compartments from each other. A solution containing 0·5 mM $CaSO_4$, 0·5 mM KNO_3 and 0·05 mM KH_2PO_4 at pH 6·0 was added to the treatment compartment, the receiver compartment and the space around the root tip. The entire assembly with the root tip was sealed with silicon grease and placed in a temperature-controlled water bath at 25 °C.

Sixty minutes after excision, the solution in the treatment compartment was replaced with fresh nutrient solution containing approximately 10 μCi $^{32}PO_4$. The solution in the receiver compartment was mixed and then sampled five times at 15-min intervals by withdrawing 400 μL of solution. When sampling was complete, the remaining 100 μL of exudation solution in the receiver compartment was removed and discarded, and then the receiver compartment was refilled with 0·5 mL of nutrient solution without ^{32}P. The solution in the treatment compartment was replaced with 0·05 % toluidine blue for 4 min to mark the root region exposed to ^{32}P. Leakage between compartments could be easily detected by movement of the toluidine blue to the receiver or leakage check chambers. Data from chambers showing any sign of compartment leakage (detected by blue dye) were discarded.

Due to the constraints of the experiment, it was not possible to measure all six genotypes on a given day. Therefore genotypes were paired for contrast in RCA abundance, one high and one low per pair. Roots from two contrasting RCA genotypes were simultaneously exposed to ^{32}P in separate chambers. One root was placed in each chamber and four replicates of each genotype were measured sequentially in each experiment. Each experiment was repeated twice, giving a total of eight replicates for each genotype. Root segments from the treatment compartment, now dyed blue, were excised and stored in 70 % ethanol for anatomical analysis. To assess ^{32}P accumulation within the root, the 10-mm segment extending from the treatment compartment to the receiver compartment (Fig. 1A) was ashed for 20 h at 500 °C. Acropetal movement of ^{32}P was checked by sampling the leakage check compartment, the nutrient solution bathing the root tip and ashed root tip samples, and no radioactivity was

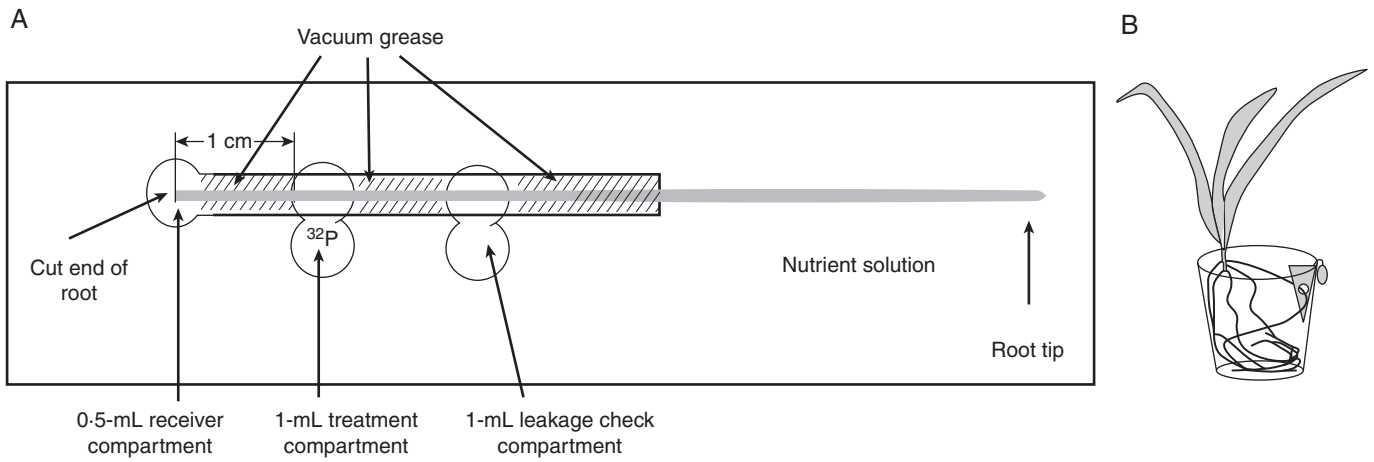

FIG. 1. Experimental setups for radionuclide application to root segments. (A) For experiment 1, a modified Pitman chamber was used to treat a 7·4-mm. segment of an excised first-whorl crown root. This top view of the acrylic glass chamber shows the 0·5 mL receiver compartment, where ^{32}P exudation from the cut end of the root was measured, the 1-mL treatment chamber where the ^{32}P was added, and the 1-mL leakage check compartment adjacent to the treatment compartment. The root tip was in a water bath containing unlabelled nutrient solution. Uptake of P was measured by adding the counts from the receiver compartment and those from the root segment inside it. (B) The chamber for experiment 2 permitted application of labelled nutrients to a 6-mm region of an intact maize seminal root. A 100-mL cup contained the whole plant, with the roots bathed in nutrient solution. One seminal root was inserted through two holes in a polypropylene tube, the openings were sealed with silicon grease and radionuclide solution was added to the tube.

found. Samples were suspended in a gelling scintillation solvent (ScintiSafe Gel Cocktail, Fisher Scientific) and analysed by liquid scintillation spectroscopy (Packard Tri-Carb 1500, Packard Instruments, Meriden, CT, USA). The counts per million (c.p.m.) for ^{32}P exudation into the receiver compartment and the c.p.m. for ^{32}P within the 10-mm root section extending from the treatment compartment to the receiving chamber were added for calculation of ^{32}P influx, i.e. these values include all ^{32}P that was taken up and transported into the treatment compartment. ^{32}P exudation refers to only the ^{32}P that moved into the receiver compartment solution.

Experiment 2: Radial transport of phosphate, calcium and sulphate by roots of whole plants. Experiment 2 was conducted to evaluate radial nutrient transport in whole plants when radiolabel was applied to small seminal root segments of varying RCA levels. Seedlings were transferred to a laboratory adjacent to the greenhouse in 100-mL cups containing nutrient solution from the solution culture tanks, covering the entire root zone (Fig. 1B). Radionuclide application chambers were constructed from a 500-µl polypropylene tube (Axygen Scientific, Union City, CA, USA) with two opposing 3-mm diameter holes in the side walls, rested on the edge of the cup by the tube lid. One seminal root from each plant was threaded through the holes in the tube and sealed with silicon grease, isolating a 6-mm length of root (the inner diameter of the tube) for exposure to radionuclides. Exposed root regions were at the basipetal end of the seminal root, 10–50 mm from the hypocotyl, and remained attached to the intact plant. The basipetal region of seminal roots was chosen for this experiment to maximize RCA variation, since in preliminary studies there was little RCA formation in sections more than 50 mm from the hypocotyl. This location also allowed consistency in the distance from the hypocotyl, which would have been greatly affected by root length if apical parts had been used. Nutrient solution (500 µL) without the element to be applied as radionuclide was added to the radionuclide application chamber for the short time (about 30 min) between sealing the root and adding the radionuclide in order to keep the root moist and to enable accurate calculation of specific activities once the radionuclide was added.

The isolated root segments were exposed to 10 µCi ^{32}P-phosphate, ^{45}Ca or ^{35}S-sulphate (MP Biomedicals, Solon, OH, USA) in 50 µL complete nutrient solution (described above for solution culture in the greenhouse). Plants were incubated under a metal halide lamp providing 150 µmol photons m^{-2} s^{-1}, the root zone being covered with aluminium foil and maintained at 25 °C by a circulating water bath surrounding the 100-mL cups. Plants from one full replicate (three treatments for three genotypes) were exposed to a single radionuclide at the same time and six replicates were used for each radionuclide, giving a total of 162 plants. After 30 min, shoots were excised, transferred to pre-weighed 20-mL scintillation vials, dried at 60 °C and weighed. Solution from the outer cup was sampled (500 µL) and dissolved in 10 mL scintillation cocktail (ScintiSafe Gel Cocktail for ^{32}P and ^{45}Ca treatments, ScintiSafe Econo Cocktail for ^{35}S treatments, Fisher Scientific) to check for radionuclide leaks from the application chamber. Samples were discarded if leaks were observed. Root regions to which radionuclide was applied were excised and stored in 25 % ethanol for later anatomical analysis. The remaining root system from each plant was then transferred to a 20-mL scintillation vial, dried at 60 °C and weighed.

Radionuclide content in the entire shoot of each plant was determined in the ^{32}P and ^{45}Ca treatments from ashed tissue (20 h at 500 °C) suspended in scintillation gel (ScintiSafe Gel Cocktail) using a liquid scintillation spectrometer (Packard Tri-Carb 1500). Radionuclide content in shoots from the ^{35}S treatment was determined according to (Naeve and Shibles, 2005). Dried shoots were pulverized in a plastic scintillation vial with a methacrylate ball in a Mixer Mill 8000 (Spex, Inc.).

Tissue was decolorized by adding 1–2 mL 6 % NaOCl and incubating for 2 h at 65 °C with vials tightly capped. Tissue was then suspended in scintillation cocktail (ScintiSafe Econo Cocktail) and counted on a liquid scintillation spectrometer with quench correction by the transformed spectral index of the external standard.

Morphological and anatomical characterization

The number of lateral roots was determined in each root segment to which radionuclide was applied, and root segments from the radionuclide-treated areas were hand-sectioned under a dissecting microscope (Nikon SMZ-U). Images of cross-sections (three per sample in experiment 1; five in experiment 2) were acquired on a compound microscope (Nikon Diaphot; 40× or 100× magnification). Images were analysed for total root cross-sectional area (RXSA), stele area (SA) and percentage of root aerenchyma area in the cortex (%RCA) using RootScan (Burton *et al.*, 2012) in experiment 1 and in GIMP v. 2·5 based on pixel number in experiment 2. Root hairs were present in some samples and were rated in experiment 2 on a scale of 0–5, where 5 is highest, considering both number and length. Root hairs were very scarce in experiment 1 and were not included in the analyses. Surface area of the exposed root segment was estimated as the surface area of a cylinder, with the length determined by toluidine blue staining, and the radius was calculated from the cross-sectional area. In experiment 1, any lateral roots that were present were just emerging, so the surface area of each lateral root was estimated as the lateral surface area of a cone, with an estimated (based on visual observation) height of 1 mm and radius of 0·5 mm, giving a total of <1 mm^2 per lateral root. The additional surface area contributed by lateral roots was found to be negligible (the maximum number of lateral roots would add less than 3 % to the surface area), so these were ignored in P efflux calculations. Lateral roots were more prevalent in experiment 2 and were quantified by counting the number of lateral roots per segment of radionuclide-treated root.

Data were analysed by linear regression, multiple regression and ANOVA using SAS 9·0 (SAS Institute Inc., Cary, NC, USA) in the first set of experiments and using SPSS v. 11 (SPSS Inc., 2005) in the second set of experiments. Data from each genotype were checked for homogeneity of variance.

RESULTS

Experiment 1: ^{32}P transport dynamics in excised root segments

Genetic variation among recombinant inbred lines was observed for root anatomy in the ^{32}P application zone (Table 1, Fig. 2). RXSA and SA were correlated ($r^2 = 0{\cdot}6826$), but the other variables, including %RCA and lateral root number (LRN), were independent of each other.

Phosphate uptake and exudation. Phosphate uptake rates varied nearly 30-fold among genotypes (Table 1). Since there was genetic variation in root diameter, which would influence the surface area from which phosphate could be taken up, uptake rates were calculated on both length and surface area bases, with similar results. Coefficients of variation for phosphate influx (pmol mm^{-2} h^{-1}) averaged 0·64. Multiple regressions showed that %RCA ($P < 0{\cdot}0001$) and LRN ($P = 0{\cdot}0024$) had significant effects on phosphate uptake, while RXSA and SA did not, despite genetic variation for these traits. There was a significant negative correlation between phosphate uptake and %RCA ($P < 0{\cdot}001$, Fig. 3). A positive relationship was observed between phosphate uptake and LRN ($r^2 = 0{\cdot}39$, $P < 0{\cdot}001$). Lateral roots did not exceed 1 mm in length. We estimated the surface area of segments bearing lateral roots using RXSA, segment length, the number of lateral roots and lateral root surface area (see Materials and methods), and found that the small lateral roots that were present would cause less than 3 % increase in surface area. The effects of lateral roots on phosphate uptake in experiment 1 were therefore not due to the increased surface area. Lateral roots were particularly abundant on RIL 321 (5–9 lateral roots) but were also present on root samples of the other genotypes (0–3 lateral roots). If RIL 321 was omitted from the analysis, there was no relationship between P uptake and LRN (data not shown).

The time course of ^{32}P exudation into the receiver chamber showed that phosphate exudation by the low-RCA genotypes RIL 321, RIL 61 and RIL 369 was markedly greater than that by the high-RCA genotypes RIL 360, RIL 345 and RIL 15 (Fig. 4). There was a delay of 15–30 min before phosphate exudation was detected. The highest rate of exudation occurred in genotype RIL 321, which had moderate RCA and high LRN (Table 1, Fig. 4). Even when only the paired comparison for which both genotypes had low LRN is considered (RIL 61

TABLE 1. *Root anatomical traits and ^{32}P uptake rates of 7·4-mm root segments of six maize RILs grown in hydroponics for 12 days in experiment 1*

Line	RCA category	RXSA (mm^2)	SA (mm^2)	%RCA	LRN (per ^{32}P-treated segment)	P uptake (pmol mm^{-2} h^{-1})
RIL 369	Low	1·77 ± 0·22 a	0·25 ± 0·06 ab	0·76 ± 0·58 c	2·17 ± 0·98 b	3·838 ± 0·687 c
RIL 15	High	1·37 ± 0·08 b	0·22 ± 0·02 b	10·24 ± 1·11 a	0·75 ± 0·50 c	0·386 ± 0·053 d
RIL 321	Low	1·38 ± 0·14 b	0·28 ± 0·04 a	2·01 ± 0·74 c	7·67 ± 1·51 a	11·118 ± 0·403 a
RIL 360	High	0·91 ± 0·20 c	0·17 ± 0·05 c	6·14 ± 1·68 b	0·67 ± 1·21 c	4·288 ± 0·461 c
RIL 61	Low	1·89 ± 0·46 a	0·29 ± 0·04 a	1·56 ± 0·52 c	0·38 ± 0·74 c	6·074 ± 1·202 b
RIL 345	High	1·32 ± 0·18 b	0·22 ± 0·02 b	6·97 ± 1·52 b	0·63 ± 0·74 c	3·978 ± 0·493 c

Values shown are means ± s.e. for RXSA, SA, %RCA and LRN.
RCA categories show the paired comparisons for simultaneous measurements.
Means within columns followed by the same letter are not significantly different ($P < 0{\cdot}05$) according to Tukey's test.

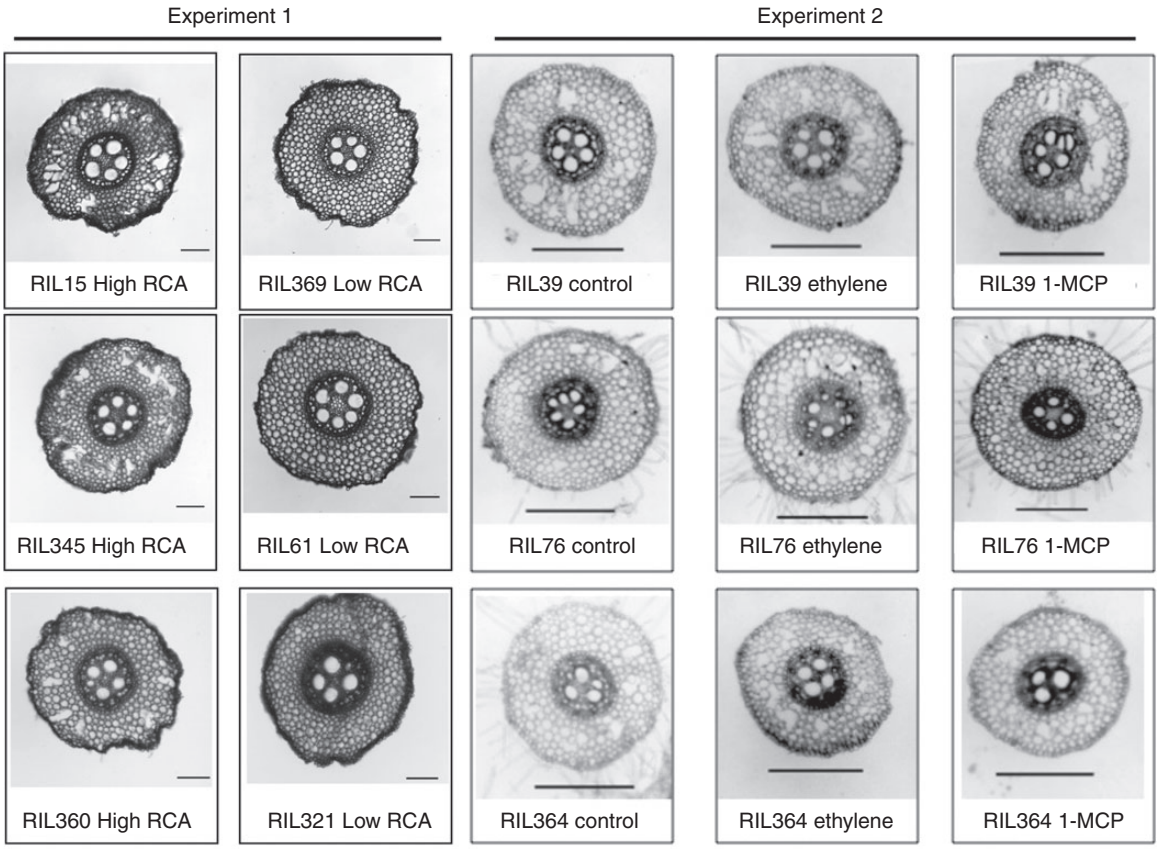

FIG. 2. Cross-sections from radionuclide-treated root segments from each genotype used in this study showing RCA formation. Images shown are representative of average RCA values for each treatment. The six images on the left are from experiment 1, where each side-by-side pair was studied at the same time, and the nine images on the right are from experiment 2, where each of the three treatments were compared at the same time. Scale bars = 400 μm.

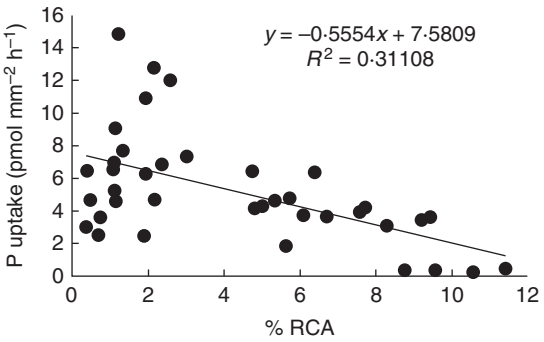

FIG. 3. Negative relationship between ^{32}P uptake and %RCA in six maize genotypes in experiment 1. The effect is significant at $P < 0{\cdot}0001$.

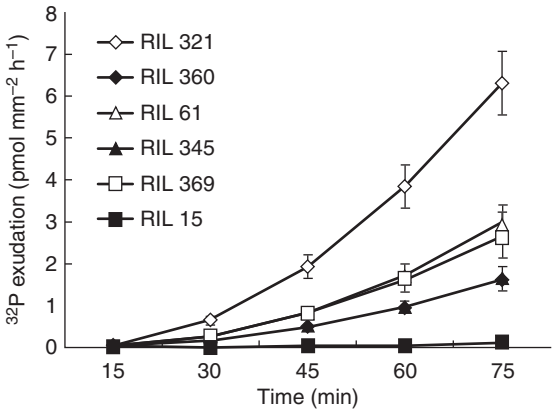

FIG. 4. Time course of cumulative ^{32}P exudation in three high-RCA genotypes (closed symbols) and three low-RCA genotypes (open symbols) in experiment 1. Error bars represent the s.e. RIL 360 is not visible because it is directly behind RIL 345.

versus RIL 345), the higher-RCA genotype, RIL 345, had a slower rate of ^{32}P exudation.

Experiment 2: radial transport of phosphate, calcium and sulphate by roots of whole plants

Plant growth and root traits. Genetic variation for several growth attributes was observed in the control treatment (Table 2). RIL 39 had the smallest dry plant mass ($P = 0{\cdot}027$), the highest level of RCA formation ($P = 0{\cdot}014$) and the lowest rating for root hair growth ($P = 0{\cdot}017$). RIL 76 had the greatest dry plant mass ($P = 0{\cdot}027$), the greatest RXSA ($P < 0{\cdot}001$), the greatest SA as a percentage of RXSA (%SA) ($P = 0{\cdot}086$), and the highest LRN in the root segment sampled ($P < 0{\cdot}001$). Trends in plant

TABLE 2. *Plant growth and root traits in maize RILs grown in solution culture with root-zone ethylene and 1-MCP treatments in experiment 2*

	Plant dry mass (g)	RXSA (mm^2)	%SA	LRN (no. per 6-mm root segment)	Root hair rating (0–5)	%RCA	LCA (mm^2)
RIL 39							
Control	0·13 ± 0·02	1·49 ± 0·11[a]	14·93 ± 0·28[a]	3·33 ± 0·55	0·22 ± 0·19	8·15 ± 1·75	1·16 ± 0·09
Ethylene	0·13 ± 0·02	1·59 ± 0·08[a]	15·49 ± 0·56[a]	2·72 ± 0·56	0·26 ± 0·13	8·65 ± 1·36	1·24 ± 0·08
1-MCP	0·13 ± 0·02	1·10 ± 0·12[b]	18·14 ± 0·44[b]	3·06 ± 0·60	0·02 ± 0·02	11·34 ± 1·30	0·79 ± 0·09
RIL 76							
Control	0·33 ± 0·03	2·03 ± 0·09	16·37 ± 0·59	7·78 ± 0·91[a]	1·12 ± 0·29	3·25 ± 1·14	1·65 ± 0·09
Ethylene	0·29 ± 0·03	1·90 ± 0·12	15·70 ± 0·58	4·78 ± 1·01[b]	0·93 ± 0·31	3·65 ± 0·90	1·54 ± 0·10
1-MCP	0·31 ± 0·04	1·73 ± 0·18	16·78 ± 0·71	4·11 ± 0·72[c]	0·92 ± 0·32	1·31 ± 0·63*	1·43 ± 0·16
RIL 364							
Control	0·17 ± 0·01	1·37 ± 0·11	15·47 ± 0·44	4·17 ± 0·35	1·20 ± 0·27	3·43 ± 0·84	1·11 ± 0·09
Ethylene	0·17 ± 0·02	1·41 ± 0·09	15·57 ± 0·42	3·72 ± 0·65	0·86 ± 0·24	5·44 ± 1·19	1·13 ± 0·08
1-MCP	0·16 ± 0·01	1·61 ± 0·11	15·39 ± 0·55	4·00 ± 0·68	1·49 ± 0·22	3·17 ± 0·81*	1·32 ± 0·09

Values are means ± s.e.; $n = 18$ in each case.
Significant differences among treatments of a given genotype as determined by one-way ANOVA are denoted by different letters.
*RCA formation in the 1-MCP treatment was significantly lower than in the ethylene treatment (*t*-test).
LCA, living cortical area calculated as total cortical area minus RCA area.

mass reflected seed mass (g) for each genotype, which was 0·202 ± 0·004 for RIL 39, 0·315 ± 0·005 for RIL 76 and 0·267 ± 0·01 for RIL 364. Root-to-shoot ratio averaged 1·20 ± 0·06 and did not differ among genotypes or treatments. In general, roots appeared to be more mature in experiment 2 than in experiment 1.

The response to ethylene and 1-MCP treatments varied with genotype (Table 2). In RIL 39, the lowest RXSA ($P = 0·005$) and the highest %SA ($P < 0·001$) were observed in the 1-MCP treatment. Treatments did not affect RCA formation in RIL 39. In RIL 76, roots in the 1-MCP treatment had significantly less RCA formation than in the ethylene treatment ($P = 0·043$) and both 1-MCP and ethylene reduced LRN ($P = 0·012$). RIL 364 roots treated with 1-MCP had less RCA than ethylene-treated roots, but this effect was significant only in roots with RXSA greater than 1·5 mm^2. Visual observations of whole root systems indicated that the 1-MCP treatment caused a lengthening of lateral roots in general. No relationship between treatment and root hair formation was observed, perhaps because root hairs formed on these segments of the roots before the seedlings were exposed to ethylene or 1-MCP.

The combination of different genotypes and treatments yielded a wide variation in abundance of RCA (Fig. 2), ranging from 1·31 % for the 1-MCP treatment of RIL 76 to 11·34 % for the 1-MCP treatment of RIL 39. Coefficients of variation for %RCA ranged from 0·48 in the 1-MCP treatment of RIL 39 to 1·91 in the 1-MCP treatment of RIL 76. The treatments affected other anatomical traits in addition to RCA; for example, 1-MCP had a tendency to reduce RXSA and increase the proportion of SA, but this was only significant in RIL 39. The coefficient of variation among the five sub-replicate cross-section images in almost all exposed root regions was <1 for %RCA, RXSA and %SA. No relationship was observed between plant mass and RCA in the 6-mm sampled root segments.

Nutrient transport. Over the 30 min uptake experiments, an average of 0·036 ± 0·008 nmol calcium, 4·31 ± 0·49 nmol phosphate and 20·4 ± 2·12 nmol sulphate was taken up by the 6-mm root segment to which radionuclide was applied and transported to the shoot. Coefficients of variation for nutrient uptake were high, with values of 2·27 for calcium, 1·12 for phosphate and 1·08 for sulphate (average coefficient of variation for the study, 1·49 ± 0·39).

When compared over all genotypes and treatments applied for each nutrient studied in experiment 2, no significant effect of RCA on radial nutrient transport was observed. However, a direct relationship was observed between nutrient transport and RCA in certain genotype and nutrient combinations (Fig. 5). For statistical analysis, a variable for classes of RXSA was created by grouping roots of <0·5 mm^2 (much less than the average area of 1·6 mm^2 and about 4 % of all samples), 0·5–1·5 mm^2 (43 % of all samples) and >1·5 mm^2 (53 % of all samples). Calcium transport was negatively related to RCA in RIL 76 ($r^2 = 0·337$, $P = 0·029$; Fig. 5A), and also in roots with a cross-section area >1·5 mm^2 in all genotypes and treatments ($r^2 = 0·124$, $P = 0·092$). Phosphate transport was negatively correlated with RCA in RIL 364 ($r^2 = 0·388$, $P = 0·017$; Fig. 5B), and also in roots with a cross-section area between 0·5 and 1·5 mm^2 ($r^2 = 0·292$, $P = 0·046$). No direct relationship between sulphate transport and RCA was observed. Other root attributes were also related to radial nutrient transport (Table 3).

Radionuclide content of a 500-μl sample from the cup solution surrounding the main root system averaged 16 ± 0·4 nCi for ^{35}Ca, 25 ± 0·5 nCi for ^{32}P and 1·18 ± 0·03 μCi for ^{45}S. Nutrient transport was correlated with radionuclide content of the cup solution sample only for sulphate ($r^2 = 0·096$, $P = 0·022$).

DISCUSSION

Formation of RCA reduced uptake rates of phosphate in 14- to 16-day-old excised roots and whole maize plants, and negative trends were observed between RCA formation and uptake of sulphate and calcium in whole plants. Although large variability in nutrient transport was observed, which was likely due to variation in RCA as well as other root attributes (Table 3), it was

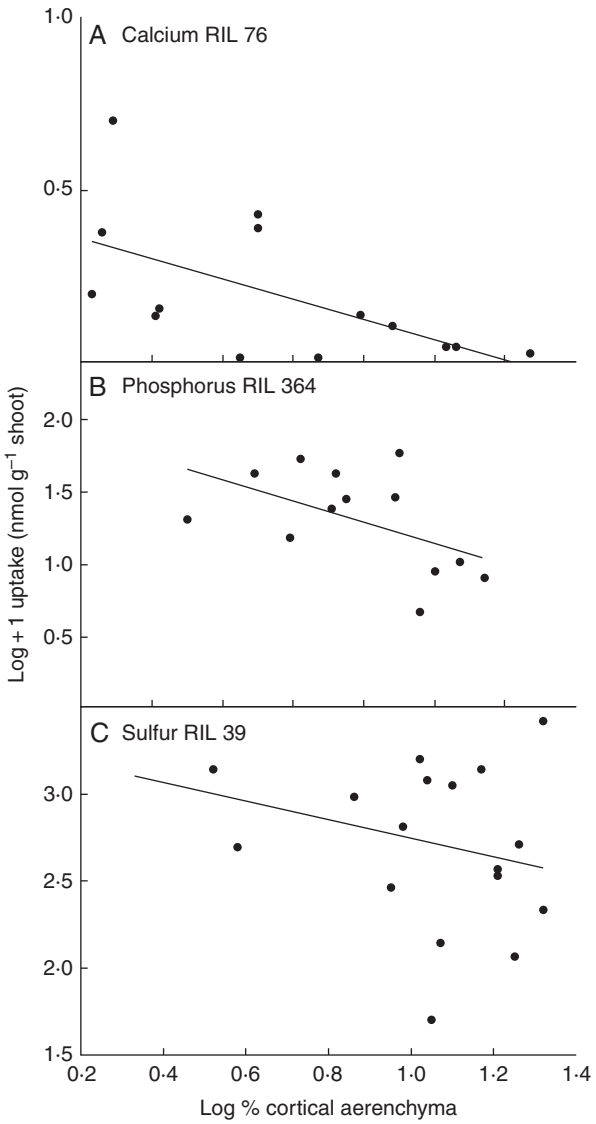

FIG. 5. Direct relationships between nutrient uptake and RCA in segments of intact maize seminal roots in experiment 2. (A) Calcium transport was negatively correlated with RCA formation in RIL 76 ($r^2 = 0{\cdot}337$, $P = 0{\cdot}029$, $y = 0{\cdot}359 - 2{\cdot}87x$). (B) Phosphate transport was negatively correlated with RCA formation in RIL 364 ($r^2 = 0{\cdot}388$, $P = 0{\cdot}017$, $y = 2{\cdot}59 - 0{\cdot}923x$). (C) A decreasing trend in sulphur transport was observed in RIL 39, although this was not significant ($r^2 = 0{\cdot}099$, $P = 0{\cdot}204$). Scale of ordinate axis is given as log + 1 to avoid negative values.

notable that no positive correlations between RCA formation and nutrient transport were observed.

Of the three nutrient ions tested, phosphate showed the most significant reduction in uptake, though calcium and sulphate uptake also tended to decline with increasing RCA (Fig. 5). Radial nutrient transport across the cortex involves both the apoplast and symplast, and nutrient ions can enter the symplastic pathway via all cell types outside the endodermis (Tester and Leigh, 2001). Sulphate and phosphate share comparable internal transport pathways, predominantly through the symplast, since they are similar in size and charge. Formation of RCA could reduce nutrient transport into the symplast by reducing the number and surface area of living cells between the epidermis and stele. Apoplastic radial pathways through the cortex would

TABLE 3. *Multiple regression models for root anatomical traits that affected nutrient transport in experiment 2*

Nutrient	Sample group	Dependent variables (y)		Independent variables	P	Regression equation	r^2
Calcium	RXSA > 1·5 mm^2	Log uptake (nmol)		Model	0·006	$y = 0{\cdot}047 - (2{\cdot}14 \times 10^{-4})a - 0{\cdot}006b$	0·416
			a	%SA	0·005		
			b	log %RCA	0·074		
	RIL 364	Log uptake (nmol g^{-1})	a	LRN	0·018	$y = 0{\cdot}386 - 0{\cdot}006a$	0·412
Phosphorus	RIL 39	Log uptake (nmol g^{-1})		Model	0·006	$y = -1{\cdot}091 + 0{\cdot}232a - 1{\cdot}041b - 0{\cdot}416c - 0{\cdot}366d - 0{\cdot}008e$	1·00
			a	%SA	0·006		
			b	Log %RCA	0·008		
			c	Root hair rating	0·010		
			d	RXSA (mm^2)	0·009		
			e	LRN	0·007		
Sulphur	RXSA = 0·5–1·5 mm^2	Log uptake (nmol)	a	LRN	0·004	$y = 0{\cdot}963 + 0{\cdot}096a$	0·327
	RXSA > 1·5 mm^2	Log uptake (nmol)	a	%SA	0·077	$y = 1{\cdot}093 + 0{\cdot}036a$	0·125

For each nutrient, the table lists sample groups for which a significant regression model was identified, as well as the root traits in the model, their significance levels (P) and the overall fit (r^2) of the model.

also be more tortuous, with fewer intercellular routes. On the other hand, if some aerenchyma lacunae are lined or filled with aqueous solution, as evidence suggests (van der Weele *et al.*, 1996), ions could diffuse along the inside of the lacunae and be taken up by cortical cells. The rate of movement of solutes towards the stele would be much faster in this case, based on dye diffusion experiments (van der Weele *et al.*, 1996). The irregularity of occurrence of these water-filled or water-lined lacunae (van der Weele *et al.*, 1996) could account for some of the variability in our nutrient transport data. The generally negative effects of RCA on nutrient transport in our experiments suggest that the tortuosity imposed by loss of cortical cells was more important than any advantage gained by water content of the lacunae.

RCA slightly reduced calcium transport, but only in larger-diameter roots when all genotypes were included in the analysis (Table 3). For individual genotypes, only RIL 76 showed significant RCA effects on calcium uptake (Fig. 5). RIL 76 also had the largest plant mass, RXSA and LCA and the lowest RCA. Since calcium intracellular homeostasis is characterized by low calcium concentrations and therefore low potential symplastic fluxes, most calcium is probably transported in the apoplast until it passes the endodermis (Clarkson, 1984; Drew and Fourcy, 1986; Halperin *et al.*, 1997), although Cholewa and Peterson (2004) concluded that radial movement of Ca^{2+} in the root occurs at least partially in the symplast. It is possible that the interruption in apoplastic flow caused by RCA was important only in the context of larger roots with longer apoplastic pathways. Interestingly, the effect of stele size on nutrient transport was positive for phosphate and sulphate but negative for calcium.

Previous studies reported that RCA does not reduce radial nutrient transport in maize (Drew and Fourcy, 1986), and may even increase it (Drew and Saker, 1986; van der Weele *et al.*, 1996). Drew and Saker (1986) measured transport of ^{32}P, ^{86}Rb and ^{36}Cl and concluded that radial transport was just as effective in aerenchymatous roots as in non-aerenchymatous roots. The movement of both Rb^+ and Sr^{2+} (as analogues of K^+ and Ca^{2+}) towards the endodermis in aerenchymatous roots was interpreted by the authors as confirmation that RCA did not reduce radial nutrient transport. Our results confirm that nutrient uptake is ongoing across the cortex of aerenchymatous maize roots. However, the previous studies induced RCA formation using a hypoxic pre-treatment, which may have had additional effects (e.g. via reduced ATP levels) on subsequent nutrient transport apart from any direct influence of RCA (e.g. Drew *et al.*, 1980; Drew and Saker, 1986). Low oxygen supply has been shown to reduce both root hydraulic conductance and ion uptake of maize grown in solution culture, and these effects were not reversible within 5 h (Birner and Steudle, 1993). We observed no effect or a negative relationship between RCA and nutrient uptake, quantified as transport to distal tissue, where variation in the amount of RCA was produced by genetic contrasts and ethylene or 1-MCP treatments. Since ethylene is a part of the normal signal transduction pathway for aerenchyma formation in maize (Drew *et al.*, 2000), its use as an RCA-inducing treatment is unlikely to cause artefacts. Therefore, the different conclusions on the effects of RCA formation on nutrient uptake between previous studies and ours appear to be attributable to a combination of interpretation of results and methodology.

Although the genotypes in this study were closely related, significant variation among genotypes was observed for growth and RCA formation. In experiment 1, using root segments, genotypes with a greater range of RCA values were used, and the impact of RCA on ^{32}P uptake and transport was highly significant. In experiment 2, only RIL 39 showed a significant effect of RCA on ^{32}P uptake (Table 3), but of the three genotypes in this study, this genotype had the highest RCA and the greatest range in RCA values (Table 2). LRN had a significant effect on phosphate transport in both sets of experiments (Table 3). For the low-RCA genotype RIL 321, which had many lateral roots in the ^{32}P treatment zone, some replicates had phosphate uptake values that were even higher than the I_{max} for phosphate uptake calculated by Bhadoria *et al.* (2004). This suggests that lateral roots played an important role in phosphate uptake, and might be an important route for phosphate loading from outside the root into the xylem of the seminal root. Furthermore, the lateral roots increased the root surface area available for phosphate uptake. Our calculations suggest that the additional surface area from these small lateral roots was not sufficient to explain the large increase in ^{32}P uptake. More likely, the lack of suberization of endodermal and hypodermal layers at the nascent root apex (Ma and Peterson, 2003; Baxter *et al.*, 2009), and possibly the disturbance of the cortical tissue caused by emergence of the lateral root (Kumpf *et al.*, 2013), could have provided high-volume pathways for nutrient uptake. Likewise, root hairs and RXSA contributed to ^{32}P uptake in experiment 2 (Table 3), most likely as a result of the increased surface area for P uptake.

In conclusion, we observed slight negative correlations between radial nutrient transport and RCA formation, and nutrient transport was highly variable due to variation in root attributes other than RCA. High-RCA genotypes had low phosphate uptake based on the time course study. Additional research is necessary in order to assess potential trade-offs of RCA for plant productivity, including studies in nutrient-deficient conditions and studies measuring RCA in the entire root system.

ACKNOWLEDGEMENTS

This research was supported by the USDA NRI Plant Biology Program grant 2007-02001. We thank Amy Burton, Claire Lorts Kirt and Larry York for their kind help during experiment 1 and Robert Snyder for support during experiment 2.

LITERATURE CITED

Baxter I, Hosmani PS, Rus A, *et al*. 2009. Root suberin forms an extracellular barrier that affects water relations and mineral nutrition in arabidopsis. *PLoS Genetics* **5**: e1000492.

Bhadoria PS, El Dessougi H, Liebersbach H, Claassen N. 2004. Phosphorus uptake kinetics, size of root system and growth of maize and groundnut in solution culture. *Plant & Soil* **262**: 327–336.

Birner T, Steudle E. 1993. Effects of anaerobic conditions on water and solute relations, and on active transport in roots of maize (*Zea mays* L.). *Planta* **190**: 474–483.

Bouranis DL, Chorianopoulou SN, Siyiannis VF, Protonotarios VE, Hawkesford MJ. 2003. Aerenchyma formation in roots of maize during sulphate starvation. *Planta* **217**: 382–391.

Burton AL, Williams MS, Lynch JP, Brown KM. 2012. RootScan: software for high-throughput analysis of root anatomical traits. *Plant & Soil* **357**: 189–203.

Cholewa E, Peterson CA. 2004. Evidence for symplastic involvement in the radial movement of calcium in onion roots. *Plant Physiology* **134**: 1793–1802.

Clarkson DT. 1984. Calcium transport between tissues and its distribution in the plant. *Plant Cell and Environment* **7**: 449–456.

Drew MC, Chamel A, Garrec J-P, Fourcy A. 1980. Cortical air spaces (aerenchyma) in roots of corn subjected to oxygen stress: structure and influence on uptake and translocation of 86rubidium ions. *Plant Physiology* **65**: 506–511.

Drew MC, Fourcy A. 1986. Radial movement of cations across aerenchymatous roots of *Zea mays* Measured by electron probe X-ray microanalysis. *Journal of Experimental Botany* **37**: 823–831.

Drew MC, Saker LR. 1986. Ion transport to the xylem in aerenchymatous roots of *Zea mays* L. *Journal of Experimental Botany* **37**: 22–33.

Drew MC, He CJ, Morgan PW. 2000. Programmed cell death and aerenchyma formation in roots. *Trends in Plant Science* **5**: 123–127.

Esau K. 1977. *Anatomy of seed plants*. New York: John Wiley.

Evans DE. 2003. Aerenchyma formation. *New Phytologist* **161**: 35–49.

Fan MS, Zhu JM, Richards C, Brown KM, Lynch JP. 2003. Physiological roles for aerenchyma in phosphorus-stressed roots. *Functional Plant Biology* **30**: 493–506.

Fan MS, Bai RQ, Zhao XF, Zhang JH. 2007. Aerenchyma formed under phosphorus deficiency contributes to the reduced root hydraulic conductivity in maize roots. *Journal of Integrative Plant Biology* **49**: 598–604.

Gunawardena AHLAN, Pearce DM, Jackson MB, Hawes CR, Evans DE. 2001. Characterisation of programmed cell death during aerenchyma formation induced by ethylene or hypoxia in roots of maize (*Zea mays* L.). *Planta* **212**: 205–214.

Halperin SJ, Kochian LV, Lynch JP. 1997. Salinity stress inhibits calcium loading into the xylem of excised barley (*Hordeum vulgare*) roots. *New Phytologist* **135**: 419–427.

He CJ, Morgan PW, Drew MC. 1996. Transduction of an ethylene signal is required for cell death and lysis in the root cortex of maize during aerenchyma formation induced by hypoxia. *Plant Physiology* **112**: 463–472.

Kumpf RP, Shi C-L, Larrieu A, *et al*. 2013. Floral organ abscission peptide IDA and its HAE/HSL2 receptors control cell separation during lateral root emergence. *Proceedings of the National Academy of Sciences of the USA* **110**: 5235–5240.

Lynch JP, Brown KM. 1998. Root architecture and phosphorus acquisition efficiency in common bean. In: Lynch JP, Deikman J. eds. *Phosphorus in plant biology: regulatory roles in ecosystem, organismic, cellular, and molecular processes.* Rockville, MD: ASPP, 148–156.

Lynch JP, Läuchli A. 1984. Potassium transport in salt-stressed barley roots. *Planta* **161**: 295–301.

Ma F, Peterson CA. 2003. Current insights into the development, structure, and chemistry of the endodermis and exodermis of roots. *Canadian Journal of Botany* **421**: 405–421.

Naeve SL, Shibles RM. 2005. Distribution and mobilization of sulfur during soybean reproduction. *Crop Science* **45**: 2540–2551.

Postma JA, Lynch JP. 2010. Theoretical evidence for the functional benefit of root cortical aerenchyma in soils with low phosphorus availability. *Annals of Botany* **107**: 829–841.

Postma JA, Lynch JP. 2011. Root cortical aerenchyma enhances the growth of maize on soils with suboptimal availability of nitrogen, phosphorus, and potassium. *Plant Physiology* **156**: 1190–1201.

Striker GG, Insausti P, Grimoldi AA, Vega AS. 2007. Trade-off between root porosity and mechanical strength in species with different types of aerenchyma. *Plant Cell and Environment* **30**: 580–589.

Tester M, Leigh R. 2001. Partitioning of nutrient transport processes in roots. *Journal of Experimental Botany* **52**: 445–57.

Van der Weele CM, Canny MJ, McCully ME. 1996. Water in aerenchyma spaces in roots. A fast diffusion path for solutes. *Plant & Soil* **V184**: 131–141.

Zhu JM, Brown KM, Lynch JP. 2010. Root cortical aerenchyma improves the drought tolerance of maize (*Zea mays* L.). *Plant Cell and Environment* **33**: 740–749.